Systems/Circuits

Na^+/K^+ ATPase α1 and α3 Isoforms Are Differentially Expressed in α- and γ-Motoneurons

Ian J. Edwards, Gareth Bruce, Charlotte Lawrenson, Laura Howe, Steven J. Clapcote, Susan A. Deuchars, and Jim Deuchars

School of Biomedical Sciences, University of Leeds, Leeds LS2 9JT, United Kingdom

The Na^+/K^+ ATPase (NKA) is an essential membrane protein underlying the membrane potential in excitable cells. Transmembrane ion transport is performed by the catalytic α subunits (α1–4). The predominant subunits in neurons are α1 and α3, which have different affinities for Na^+ and K^+, impacting on transport kinetics. The exchange rate of Na^+/K^+ markedly influences the activity of the neurons expressing them. We have investigated the distribution and function of the main isoforms of the α subunit expressed in the mouse spinal cord. NKAα1 immunoreactivity (IR) displayed restricted labeling, mainly confined to large ventral horn neurons and ependymal cells. NKAα3 IR was more widespread in the spinal cord, again being observed in large ventral horn neurons, but also in smaller interneurons throughout the dorsal and ventral horns. Within the ventral horn, the α1 and α3 isoforms were mutually exclusive, with the α3 isoform in smaller neurons displaying markers of γ-motoneurons and α1 in α-motoneurons. The α3 isoform was also observed within muscle spindle afferent neurons in dorsal root ganglia with a higher proportion at cervical versus lumbar regions. We confirmed the differential expression of α subunits in motoneurons electrophysiologically in neonatal slices of mouse spinal cord. γ-Motoneurons were excited by bath application of low concentrations of ouabain that selectively inhibit NKAα3 while α-motoneurons were insensitive to these low concentrations. The selective expression of NKAα3 in γ-motoneurons and muscle spindle afferents, which may affect excitability of these neurons, has implications in motor control and disease states associated with NKAα3 dysfunction.

Introduction

The Na^+/K^+ ATPase (NKA) is ubiquitously expressed in membranes and maintains ionic gradients through the antiport of Na^+ and K^+ ions. Transmembrane ion transport is performed by the catalytic α subunit, of which there are 4 isoforms (α1–4). These isoforms have different kinetic properties (Segall et al., 2001) and very specific tissue distributions (for review, see Sweadner, 1989), with potential impact on control of neuronal function. The predominant CNS subunits are the α1, α2, and α3 subunits (Sweadner, 1989; Viola and Rodríguez de Lores Arnaiz, 2007). The α1 and α3 subunits appear to be the most prominently expressed in neurons (Mata et al., 1991; Watts et al., 1991), but their expression patterns are not fully elucidated.

Understanding the expression patterns of the different isoforms of NKAα subunits has clinical implications. Two movement disorders are caused by different missense mutations in the ATP1A3 gene encoding the α3 subunit of the Na^+/K^+-ATPase (NKAα3): Alternating Hemiplegia of Childhood (AHC, OMIM #614820), characterized by episodes of transient hemiplegia/hemiparesis, dystonia and choreoathetosis (Heinzen et al., 2012; Rosewich et al., 2012; Kirshenbaum et al., 2013), and Rapid-Onset Dystonia-Parkinsonism (RDP, dystonia 12, OMIM #128235), characterized by abrupt onset of dystonia with parkinsonism after a stressful event, typically in late adolescence or early adulthood (Brashear et al., 1998; de Carvalho Aguiar, 2004; Brashear et al., 2007). The pathophysiology of RDP differs from dystonia and Parkinson's disease since L-DOPA treatment (Brashear et al., 2007) and deep brain stimulation of the basal ganglia (Deutschländer et al., 2005) have little or no therapeutic effect. Poor responses to these therapies suggest that dysfunction in motor circuits outside the basal ganglia contribute to RDP symptoms. Since the common mutation underlying these two movement disorders is in the NKAα3 subunit and given that the final common pathway for motor control is through neuronal circuitry in the spinal cord, the expression pattern of this and other NKA subunits in these spinal cord circuits may be of critical importance in understanding these pathologies.

Within the spinal cord, there is controversy regarding the specific distribution of the α1 subunit with suggestions using immunohistochemistry that it is limited to glial cells in the ventral white matter and absent from the gray matter entirely (McGrail et al., 1991), whilst *in situ* hybridization suggests that it is present within motoneurons and not in glia (Mata et al., 1991; Watts et al., 1991; Sayers et al., 1994). The α3 subunit may have a more widespread distribution, being observed within all neurons of the spinal cord including the motoneurons reported to express α1 (Mata et al., 1991). It is important

Received Dec. 6, 2012; revised March 28, 2013; accepted April 29, 2013.

Author contributions: S.J.C., S.A.D., and J.D. designed research; I.J.E., G.B., C.L., and L.H. performed research; I.J.E. analyzed data; I.J.E., S.A.D., and J.D. wrote the paper.

This work was supported by the Bachmann-Strauss Dystonia & Parkinson Foundation, Wellcome Trust (WT093072MA) and Biotechnology and Biological Sciences Research Council (BB/F006594/1). We thank Mukti Singh, Bethan Jones, and Helen Schofield for technical assistance.

This article is freely available online through the *J Neurosci* Author Open Choice option.

Correspondence should be addressed to Susan A. Deuchars, School of Biomedical Sciences, University of Leeds, Leeds LS2 9JT, UK. E-mail: S.A.Deuchars@leeds.ac.uk.

DOI:10.1523/JNEUROSCI.5584-12.2013

 0270-6474/13/339913-07$15.00/0

to resolve the tissue distribution of these isoforms and determine whether they are coexpressed within single populations of cells.

We show that NKAα subunits have a mutually exclusive expression within α- and γ-motoneurons that may represent a novel therapeutic avenue for pathologies involving motoneuron dysfunction. Furthermore, these data reveal how NKAα3 loss-of-function mutations could contribute to dysfunction in spinal circuitry and thus the motor symptoms of AHC and RDP.

Materials and Methods

All procedures were performed in accordance with the UK Animals (Scientific Procedures) Act 1986.

Immunohistochemistry. Tissue from young adult wild-type C57BL/6 mice of either sex (6 d old, $n = 3$; 6–8 weeks old, $n = 12$) was prepared for immunohistochemistry as previously described (Edwards et al., 2007). Motor, preganglionic, and sensory neurons were labeled by intraperitoneal injection of hydroxystilbamidine (Fluorogold, FG, 0.1 ml of 1% i.p. in H_2O, Fluka, BioChemika) 3 d before perfusion. Before primary antibody incubation, tissue sections were incubated in 10 mM sodium citrate at 70°C for 20 min. All primary antibody incubations were performed overnight at 4°C in PBS containing 0.1% Triton X-100 and secondary antibody incubations were performed at room temperature in PBS for 1–3 h (Invitrogen Alexa Fluor secondaries) or 4 h (Jackson ImmunoResearch biotinylated secondaries).

Tissue sections were incubated with rabbit anti-NKAα3 (1:500–1000; Millipore Biotechnology), or mouse anti-NKAα3 (1:1000; Affinity Bioreagents) and detected using donkey anti-rabbit Alexa Fluor 555 (1:1000, Invitrogen) or donkey anti-mouse Alexa Fluor 488 (1:1000, Invitrogen) as appropriate. NKAα1 was detected with monoclonal antibodies raised in rabbit (Epitomics, 2047-1, 1:1000) or mouse (DSHB, 6F, 1:100), visualized with Alexa Fluor-conjugated secondary antibodies appropriate to double labeling protocols.

Western blotting. Protein extraction and blot analysis. Membrane protein fractions were isolated from frozen spinal cord and brain tissue from C57BL/6 mice using a ProteoJET Membrane Protein Extraction Kit (Fermentas) according to the manufacturer's instructions. Twenty-four micrograms of each membrane extract, determined by Bradford assay (Protein Assay, Bio-Rad), were incubated at 37°C for 15 min, subjected to gradient SDS-PAGE (100 V, 1.5 h) in 4–15% Mini-PROTEAN TGX Gels (Bio-Rad) in parallel with 5 μl Precision Plus Protein Standard (Bio-Rad), and then blotted (100 V, 2 h) onto PVDF membrane (Pall). After blocking with 5% milk in PBS-T (PBS, 0.1% Tween-20) overnight, membranes were incubated for 2 h with rabbit anti-NKA α1 (Epitomics; 1:10,000) or rabbit anti-NKA α3 (06–172; Millipore; 1:1000). Immune complexes were detected by chemiluminescence (Novex ECL, Invitrogen) with HPR-conjugated chicken anti-rabbit (Santa Cruz Biotechnology; 1:2000). Protein bands were visualized by exposing the membranes to photographic film for 30 s.

Anti-NKA antibody specificity. Western blots of mouse brain and spinal cord using the rabbit anti-NKAα1 antibody, raised against an N-terminal peptide sequence unique to the α1 isoform, detected a single band with a molecular weight of ~100 kDa (Fig. 1), consistent with the molecular weight of this isoform in rat brain preparations (Shyjan and Levenson, 1989). We further confirmed the specificity of antibody staining for NKAα1 using the monoclonal antibody 6F (DSHB). This antibody (6F) has previously been indicated to be specific to NKAα1 by extensive Western blotting and epitope mapping in several tissues of different species, where it was also shown that it did not cross react with NKAα2 or NKAα3 (Arystarkhova and Sweadner, 1996).

The Millipore antibody to NKAα3 (raised against a fusion protein of amino acids 320–514 of the NKAα3) has been extensively characterized as specific previously, where Western blotting showed that it detected a single protein of ~100 kDa corresponding to the molecular weight of the α subunit of NKA in lysate from whole brain or neurons (Shyjan and Levenson, 1989). Western blots of brain and spinal cord revealed a single band with a molecular weight of ~100 kDa from both tissues (Fig. 1). The mouse anti-NKAα3 antibody (Affinity Bioreagents, clone XVIF9-G10) detects a sequence within 50 aa of the N terminus as shown by epitope mapping and its lack of reactivity with NKAα1 and NKAα2 and specificity has previously been shown by Western blotting (Arystarkhova and Sweadner, 1996).

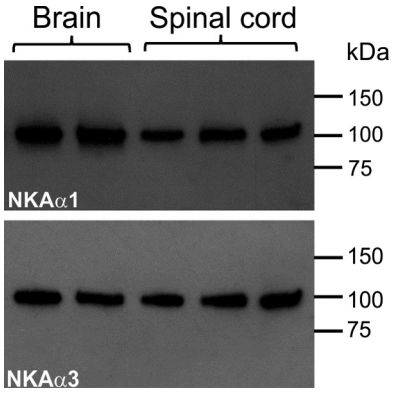

Figure 1. Western blot analysis of the specificity of NKAα1 and α3 antibodies. Brain and spinal cord homogenates were probed with antibodies raised against either NKAα1 or NKAα3. Both antibodies recognized a single band in all homogenates.

Neurochemical characterization. To detect motoneurons, double labeling was performed using goat anti-choline acetyltransferase (ChAT; 1:500, AB144P, Millipore), which was visualized using donkey anti-goat Alexa Fluor 488 (1:1000, Invitrogen). To distinguish between α- and γ-motoneurons, α3 and ChAT immunohistochemistry were combined with staining for NeuN, which is absent from γ-motoneurons (Friese et al., 2009), using mouse anti-NeuN (1:1000, Clone A60, Millipore), detected using biotinylated secondary antibodies (donkey anti-mouse 1:250, Jackson ImmunoResearch) and streptavidin Pacific Blue (1:1000 in PBS, Invitrogen).

To determine whether α3 was found within the large muscle spindle afferent neurons, double labeling was performed upon 50 μm sections of dorsal root ganglion (DRG) for parvalbumin (Pv; mouse anti-Pv, 1:1000, P3088, Sigma).

Tissue was then prepared for viewing using a Nikon E600 epifluorescent microscope and Acquis image capture system (Synoptics) or an Inverted Zeiss LSM510 confocal microscope.

Electrophysiology. Spinal cord slices from neonatal mice (6–11 d, $n =$ 10 mice) were prepared as previously described for rats (Wang et al., 2008). Whole-cell current-clamp recordings were made from large ventral horn neurons. Through the addition of tetramethylrhodamine and neurobiotin to the intracellular solution, recorded neurons were confirmed as motoneurons upon *post hoc* analysis of their morphology. Neurons were held at ~−60 mV and characterized by injection of rectangular hyperpolarizing and depolarizing current pulses of −300 to +500 pA (1 s duration). Data analysis was performed off line. To further distinguish between α- and γ-motoneurons, recorded cells were tested for their sensitivity to the 5HT-1D agonist L694247, the receptor for which is selectively expressed in γ-motoneurons (Enjin et al., 2012). All cells were tested for responses to 3 μM ouabain, a cardiac glycoside that inhibits NKAα3 in the nM-μM range (Urayama and Sweadner, 1988). Cells that did not respond to 3 μM ouabain were then tested with 30 μM ouabain to reveal responses mediated by NKAα1.

Statistical analysis. All data are presented as mean ± SEM, and significance was set at $p < 0.05$. For immunohistochemistry experiments, n refers to the number of animals and N refers to the number of cells counted; for electrophysiological experiments, n refers to the number of cells recorded. For both immunohistochemical and electrophysiological data, significance was tested using unpaired Student's t test to examine differences between α- and γ-motoneurons.

Results

Distribution of NKAα1 in the spinal cord

NKAα1 immunoreactivity was observed in cervical, thoracic, and lumbar spinal cord sections ($n = 7$, Fig. 2*A*–*A*2). NKAα1 immu-

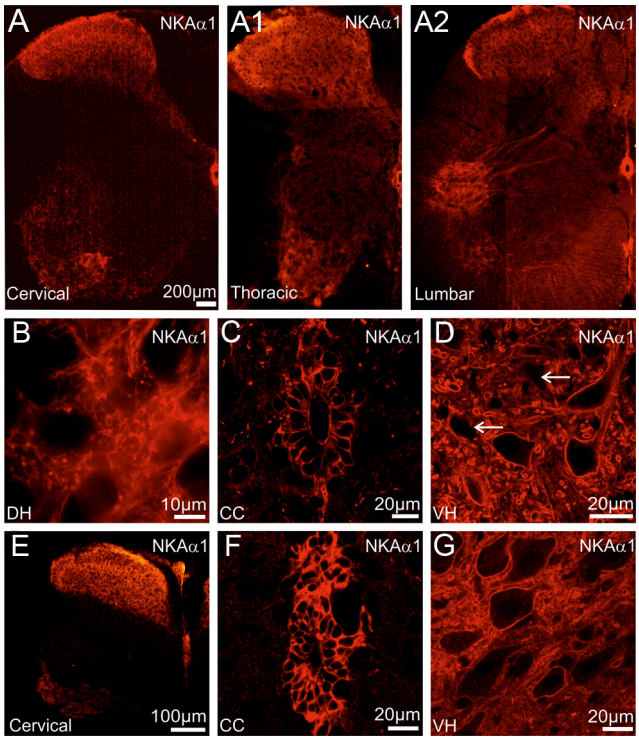

Figure 2. NKAα1 immunoreactivity is observed within motoneurons in the spinal cord. NKAα1 immunoreactivity displays the same pattern across all levels of the spinal cord (***A–A2***). Within the superficial laminae of the dorsal horn, fine fibers and puncta are immunoreactive for NKAα1 (***B***). In lamina X, close to the central canal, NKAα1-IR is absent from neurons and is expressed strongly in the membranes of the ependymal cells surrounding the central canal (***C***). Within the ventral horn, NKAα1-IR is only found in the membranes of large presumed α-motoneurons, with smaller NKAα1-IR-devoid neurons indicated with arrows (***D***). The staining pattern observed at postnatal day 6 (***E–G***) closely resembles that observed in the adult. DH, Dorsal horn; VH, ventral horn; CC, central canal.

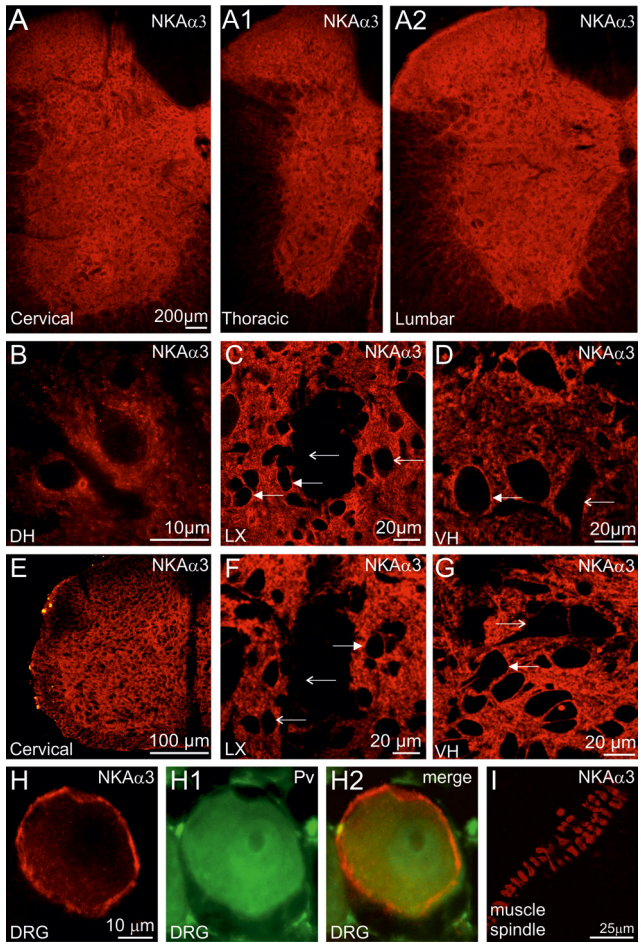

Figure 3. NKAα3 immunoreactive neurons can be observed throughout the spinal cord and in a subpopulation of DRG neurons. NKAα3 immunoreactivity is more ubiquitous than NKAα1-IR, with immunoreactivity throughout the neuropil at all levels of the spinal cord (***A–A2***). Within the deeper laminae of the dorsal horn, NKAα3-IR is observed in punctate structures (***B***). Within lamina X close to the central canal, NKAα3-IR is observed throughout the neuropil, with some immunoreactive neurons visible (***C***). In the ventral horn of the spinal cord, NKAα3-IR can be found in close proximity to neurons. The smaller neurons appear to have more NKAα3-IR enriched around their membranes (***D***). At postnatal day 6 (***E–G***), the pattern of immunoreactivity appears identical to that observed in the adult. In dorsal root ganglia, NKAα3-IR was observed within a proportion of the parvalbumin expressing large neurons (***H–H2***). Consistent with this, NKAα3-IR could also be observed within the membranes of muscle spindles (***I***). Examples of NKAα3-IR and NKAα3-IN neurons are marked with closed and open arrows, respectively. DH, Dorsal horn; VH, ventral horn; LX, lamina X; DRG, dorsal root ganglion.

noreactivity (IR) was found within putative presynaptic structures within the superficial layers of the dorsal horn (Fig. 2*B*). The ependymal cells surrounding the central canal (CC) were strongly immunopositive for NKAα1 (Fig. 2*C*), as were neurons in the ventral horn (Fig. 2*D*). In the lateral horn, NKAα1-IR was visible in the membranes of neurons (Fig. 2*A*1) that were identified as sympathetic preganglionic neurons as they were also choline acetyltransferase (ChAT) positive (data not shown). The pattern of staining did not differ between 6 d (the age at which electrophysiology is performed) and 6–8 weeks (Fig. 2*E–G*).

Distribution of NKAα3 in the spinal cord

NKAα3-IR was also observed throughout the spinal cord at cervical, thoracic, and lumbar levels ($n = 12$, Fig. 3*A–A2*). All areas of the spinal cord displayed immunoreactivity for NKAα3. However, upon closer examination, it was observed that this NKAα isoform is not ubiquitously expressed; rather, NKAα3-IR was concentrated in the membranes of some cells and absent from others. This was particularly clear within lamina X of the spinal cord, where NKAα3-IR could be seen in the membranes of small to medium sized neurons but was absent from ependymal cells (Fig. 3*C*). In the dorsal horn, the larger neurons within this region were also NKAα3-immunonegative, although surrounded by NKAα3-IR punctate structures (Fig. 3*B*). This pattern was observed again in the ventral horn, where many cells were immunoreactive for NKAα3, but approximately two thirds of the large cells (presumed α-motoneurons) were devoid of immunoreactivity (Figs. 3*D*, 4). Again, the pattern of staining was not different between the two ages studied (Fig. 3*E–G*).

NKAα1 and NKAα3 subunits are found within distinct populations of motoneurons in the ventral horn

Ventral horn motoneurons, identified through immunoreactivity for ChAT (Fig. 4*A*2) and retrograde tracing from the periphery with Fluorogold (Fig. 4*A*3), were immunopositive for either the NKAα1 OR the NKAα3 subunit but never both and this selectivity correlated with soma size (Fig. 4*A–A*4). Specifically, the NKAα1-immunopositive motoneurons were significantly larger than those that expressed the NKAα3 subunit (NKAα1-IR $1439 \pm 89\ \mu m^2$, $N = 91$ vs NKAα3-IR $333 \pm 16\ \mu m^2$, $N = 48$, $n = 5$; Fig. 4*A*5, $p < 0.001$). The separation of the expression of either NKAα1 or NKAα3 on the basis of size suggests that the NKAα1 subunit is found within α-motoneurons and that NKAα3 subunit is expressed by γ-motoneurons. To confirm that

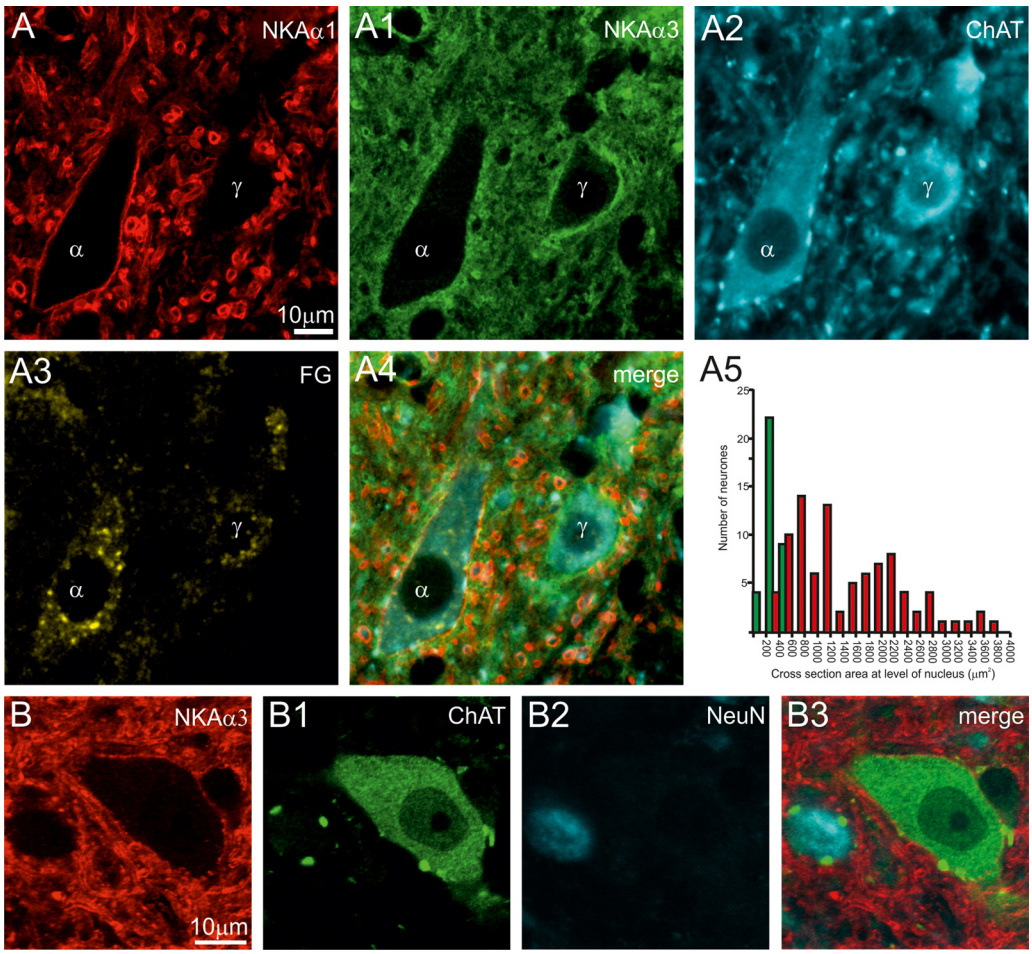

Figure 4. NKAα3 is found in small γ-motoneurons, while larger α-motoneurons express NKAα1. Immunoreactivity for NKAα1 and NKAα3 reveals two distinct populations of motoneurons within the ventral horn (***A–A5***). Neurons were confirmed as motoneurons through the expression of ChAT (***A2***) and retrograde labeling from the periphery with Fluorogold (***A3***). Measuring the area of the motoneurons expressing either NKAα1 (***A5***, red bars) or NKAα3 (***A5***, green bars) reveals two distinct populations of neurons based upon size. The likelihood of the small motoneurons immunoreactive for NKAα3 being γ-motoneurons was strengthened through the absence of NeuN within these neurons (***B–B3***).

the small NKAα3-IR motoneurons were γ-motoneurons, we assessed the expression of NeuN in conjunction with immunohistochemistry for the two NKAα isoforms. NeuN is found within α-motoneurons but is absent from γ-motoneurons (Friese et al., 2009). NeuN expression was absent from NKAα3-IR motoneurons, confirming them as γ-motoneurons (Fig. 4*B–B3*).

NKAα3 subunits are also found within the sensory components of the fusimotor system

We next determined whether the NKAα3 subunit was expressed in the muscle spindle afferents that make up the sensory part of the fusimotor system. Consistent with previous findings, NKAα3-IR was only observed in a subpopulation of dorsal root ganglion neurons (Dobretsov et al., 1999; Romanovsky et al., 2007). Interestingly, there appeared to be significantly more NKAα3-IR neurons in cervical DRG (C4, 73.1 ± 5.0%, N = 311/433, n = 7) than in lumbar (L2, 17.2 ± 2.8%, N = 131/773, n = 6, p = 0.00002). At both lumbar and cervical levels, the NKAα3-IR neurons were large and double-labeling for parvalbumin (Pv), a marker for muscle sensory afferents (Arber et al., 2000; Ichikawa et al., 2004; Mentis et al., 2006) (Fig. 3*H–H2*), revealed that without exception, all NKAα3-IR neurons were also Pv-IR. To confirm further that these sensory neurons were muscle spindle afferents, we performed immunohistochemistry for NKAα3 on muscle sections, in which clear NKAα3-IR was found throughout the membrane of the spindle afferent wrapping around the intrafusal muscle fiber but not within the fiber itself (N = 17, n = 4; Fig. 3*I*).

Low concentrations of ouabain depolarized γ-motoneurons but not α-motoneurons, suggesting that functional NKAα3 subunits are limited to γ-motoneurons

Whole-cell patch-clamp recordings were undertaken in mouse spinal cord slices. Large neurons in the ventral horn, targeted as putative motoneurons, were filled with rhodamine and neurobiotin and confirmed as such *post hoc* (Fig. 5*A*,*B*). Motoneurons typically had a large soma, an axonal projection heading ventrally toward the edge of the gray matter and a multipolar arrangement of dendrites. Discrimination of α- and γ-motoneurons based solely on their size is not appropriate at this age, since there is a high degree of overlap between the cell cross-sectional areas of the two classes of motoneuron (Shneider et al., 2009), and was therefore not used as a factor to differentiate between the two classes. Motoneurons had very low input resistance in keeping with their large somatic size, and a high rheobase. On the basis of their responses to hyperpolarizing and depolarizing current pulses, motoneurons were putatively split into α (n = 5) and γ (n = 8) subtypes. Consistent with previous reports (Enjin et al., 2012), γ-motoneurons had a higher input resistance than α-motoneurons (180 ± 52 vs 78 ± 15 MΩ, p < 0.05).

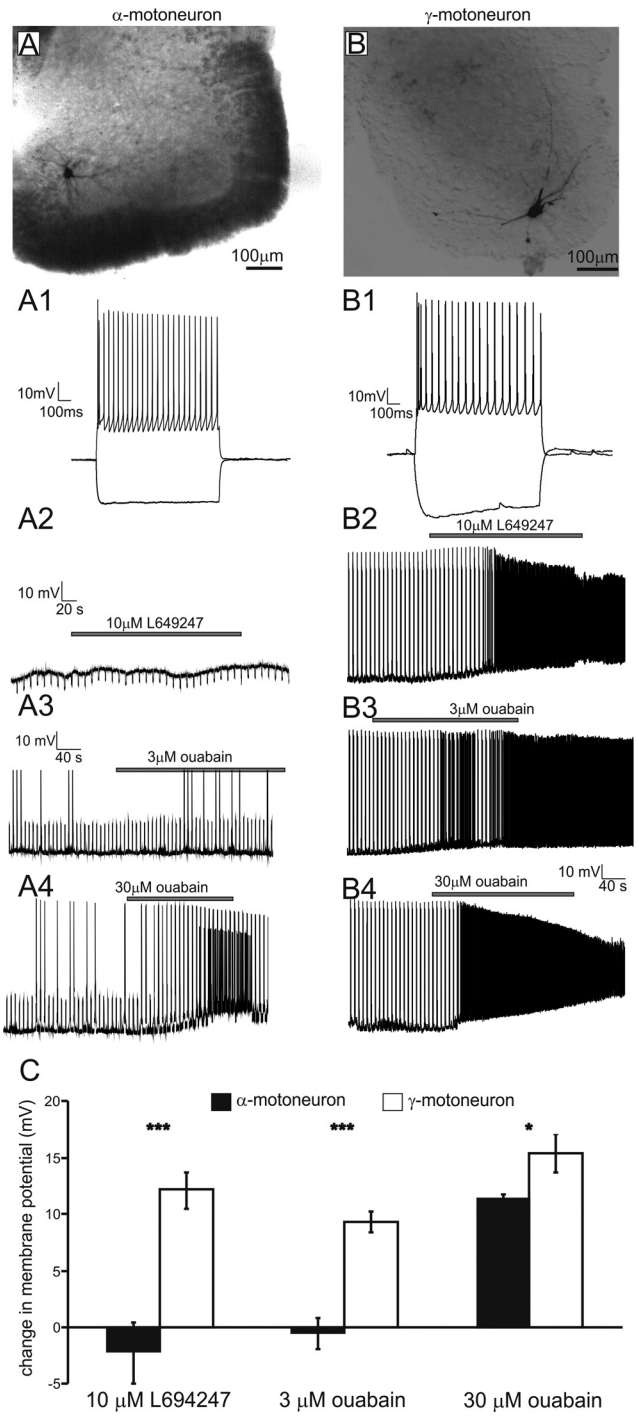

Figure 5. γ-Motoneurons are sensitive to lower concentrations of ouabain than α-motoneurons. Electrophysiological recordings were made from cells confirmed as motoneurons by their morphology (***A***, ***B***) and their basic electrophysiological responses to depolarizing and hyperpolarizing current pulses (***A1***, ***B1***). Cells were confirmed as either α- or γ-motoneurons based upon and their response to the 5HT1D agonist L694247 (10 μM, ***A2*** and ***B2***, $n = 5$ and 8, respectively). γ-Motoneurons, which responded to L694247, also responded to 3 μM ouabain (***B3***, $n = 8$) and 30 μM ouabain (***B4***, $n = 3$). α-Motoneurons, which did not respond to L694247, did not respond to 3 μM ouabain (***A3***, $n = 5$) but did respond to 30 μM ouabain (***A4***, $n = 5$). Group data comparing these responses is shown in ***C***, black bars = α-motoneurons and white bars = γ-motoneurons. $^*p < 0.05$, $^{**}p < 0.01$, $^{***}p < 0.005$.

α-Motoneurons also displayed a more negative action potential threshold than that observed in γ-motoneurons (−43.4 ± 1.9 vs −31.8 ± 4.6 mV, $p < 0.05$) and a longer action potential duration (4.9 ± 0.6 vs 3.5 ± 0.3 ms, $p < 0.05$). There were no significant differences observed in the resting membrane potential of the α- and γ-motoneurons (−56.3 ± 2.7 vs −61.6 ± 0.6 mV, respectively), the action potential amplitude (57.7 ± 6.1 vs 56.4 ± 5.2 mV), the amplitude of the after-hyperpolarization (4.7 ± 1.7 vs 3.8 ± 0.7 mV), the rheobase for generating action potentials (236.2 ± 84.2 vs 344.4 ± 98.0 pA), nor the delay to action potential generation at rheobase (140.1 ± 72.2 vs 169.6 ± 32.6 ms). Typical responses to hyperpolarizing and depolarizing current pulses are shown in Figure 5, *A*1 (α-motoneuron) and *B*1 (γ-motoneuron).

The classification of recorded motoneurons as α- or γ-motoneurons was ratified through bath application of the 5HT1D agonist L694247 at 10 μM (Enjin et al., 2012). L694247 evoked a robust depolarization of 15.5 ± 1.7 mV from −60 mV ($n = 7$) in those neurons classified as γ-motoneurons, but had no effect on those classified as α-motoneurons (change in membrane potential of −2.4 ± 2.7 mV, $n = 5$; Fig. 5*A*2,*B*2).

There was a highly significant difference between α- and γ-motoneurons ($p < 0.001$) in their response to 3 μM ouabain [which would strongly inhibit NKAα3 as it has an IC50 for ouabain of ~6.7 nM, but not inhibit NKAα1-IC50 for ouabain is 38 μM (O'Brien et al., 1994)], with γ-motoneurons displaying a clear depolarization (9.4 ± 0.9 mV, time to peak 311.6 ± 74.0 s, $n = 8$) and α-motoneurons displaying no change in their membrane potential (−0.55 ± 1.4 mV, $n = 5$; Fig. 5*A*3,*B*3). There were also significant differences in the response of α- and γ-motoneurons to 30 μM ouabain (which, based on the IC50 values above, would strongly inhibit NKAα3 and would inhibit NKAα1 to a lesser extent). α-Motoneurons depolarized by 11.4 ± 0.5 mV to bath application of 30 μM ouabain ($n = 5$), while γ-motoneurons displayed a greater depolarization of 15.5 ± 1.7 mV ($n = 3$, $p < 0.05$; Fig. 5*A*4,*B*4). The response to 30 μM ouabain in α-motoneurons was also slower than that observed in γ-motoneurons (time to peak 293.7 ± 71.5 vs 136.5 ± 26.0 s, $p < 0.05$). Group data for drug responses is summarized in Figure 5*C*.

Discussion

This study applies both immunohistochemistry and electrophysiology to explore the distribution of NKAα1 and NKAα3 subunits in motoneurons of the spinal cord. Strikingly, the subunits are differentially expressed in motoneurons, as the NKAα1 is present in α-motoneurons, whereas the NKAα3 is restricted to γ-motoneurons. Furthermore, consistent with a primary role on proprioception in the motor system, NKAα3 is also present in parvalbumin-positive sensory neuron somata and sensory endings in the muscle spindle. Electrophysiological recordings from ventral horn motoneurons confirm the presence of NKAα3 in γ-motoneurons and NKAα1 in α-motoneurons.

We report a widespread localization of NKAα3 in the spinal cord but it appears absent from α-motoneurons. The restriction of NKAα3 to γ-motoneurons is consistent with immunostaining of ventral roots, where NKAα3 immunoreactivity is only found in the smaller caliber axons, and also staining of muscle where NKAα3 is found in end plates on intrafusal muscle fibers (Romanovsky et al., 2007). Here, we also show that NKAα1 is expressed prominently in large ventral horn neurons. These we have defined as α-motoneurons on the basis of their expression of ChAT and NeuN (Friese et al., 2009). To functionally confirm the differential distribution of NKAα1 and NKAα3 subunits to α- and γ-motoneurons, respectively, we exploited the differing sensitivity of these isozymes to the cardiac glycoside ouabain. Only motoneurons sensitive to the 5HT1D agonist L694247 also

responded to a low micromolar concentration of ouabain, consistent with the specific localization of the NKAα3 subunit to γ-motoneurons. Motoneurons which were insensitive to L694247 did, however, respond to a much higher concentration of ouabain, sufficient to inhibit the NKAα1 subunit. This demonstrates a clear difference in the sensitivity of α- and γ-motoneurons to exogenously applied ouabain, consistent with the differential expression of NKAα subunits.

We found that NKAα3-IR cells had smaller somata than NKAα1-IR cells, consistent with previous studies that γ-motoneurons have smaller soma size than α-motoneurons (Strick et al., 1976; Westbury, 1982). Furthermore, NKAα3-IR motoneurons did not express NeuN, another property that differentiates γ-motoneurons from α-motoneurons (Friese et al., 2009). Thus, NKAα3 expression can be added to the growing markers that can be used to differentiate γ-motoneurons from α-motoneurons, such as ERR3 (Friese et al., 2009) and GDNF (glial cell line-derived neurotrophic factor) receptor subunit GFRα1(Shneider et al., 2009) and 5HT 1D receptors (Enjin et al., 2012).

We found the NKAα3 subunit expressed within parvalbumin-positive sensory neurons and muscle spindle sensory endings, previously linked with proprioceptive functions (Dobretsov, 2003; Romanovsky et al., 2007). We also noted that the proportion of NKAα3-expressing neurons is higher in cervical DRG than in lumbar. This indication that there is a higher proportion of cervical DRG neurons with potential proprioceptive function than lumbar DRG neurons is supported by the observation that up to 65% of cervical DRG neurons project to the dorsal column nuclei compared with15% of lumbar DRG neurons in the rat (Giuffrida and Rustioni, 1992). Although it must be noted that not all dorsal column nuclei projecting neurons are involved in proprioception, these proportions tally well with those of the NKAα3-positive sensory neurons in this study. Presumably, this increased proprioceptive traffic at cervical levels reflects high levels of dexterity and degrees of movement in the hands, forelimbs, and high muscle spindle content of neck muscles (Richmond and Abrahams, 1975; Kulkarni et al., 2001).

The physiological relevance of selective expression of NKAα subunits in neurons remains to be fully determined. However, the NKAα3 subunit is able to extrude Na^+ ions that accumulate intracellularly during action potential firing at a faster rate than NKAα1, which supports higher firing rates of neurons (Azarias et al., 2013). This is consistent with higher firing rates observed in γ-motoneurons than α-motoneurons both *in vivo* (Ellaway and Murphy, 1981) and *in vitro* [here and the study by Enjin et al. (2012)]. The selective expression of NKAα3 in muscle spindle afferents peripherally is likely to be of further physiological importance, placing this exquisitely ouabain-sensitive form of the NKA throughout the fusimotor system. This system is thus likely to be selectively and tonically influenced by the adrenocortically produced hormone known as endogenous ouabain (EO), present in the circulation in the nanomolar range (Harwood and Yaqoob, 2005), which is sufficient to inhibit NKAα3 rather than NKAα1. As low concentrations of ouabain increased firing rates of γ-motoneurons in spinal cord slices, both spindle afferents and γ-motoneurons are likely to be more excitable *in vivo* due to EO. Since there is a paucity of information on the firing properties of γ-MNs in the spinal cord *in vivo*, these current data reveal a mechanism through which the excitability of γ-MNs can be regulated differentially to that of α-MNs.

Indeed, the loss of function mutation of NKAα3 in the movement disorders AHC and RDP (de Carvalho Aguiar, 2004; Brashear et al., 2007; Heinzen et al., 2012; Rosewich et al., 2012; Kirshenbaum et al., 2013) exaggerates the outcomes of NKAα3 inhibition that may be normally undertaken by EO. Current understanding of RDP suggests that the loss of function of NKAα3 in the basal ganglia and cerebellum underlies the symptoms of the disease, as dual perfusion of ouabain into these areas of the mouse brain mimics much of the phenotype of the disease (Calderon et al., 2011). Our results suggest an additional contribution to motor symptoms of AHC and RDP from dysfunction in spinal sensorimotor circuits. The loss of function mutations in NKAα3 may cause the affected spindle afferents and γ-motoneurons to exist in a more depolarized state and thus increase their excitability. In turn, it is then feasible that this would have an indirect effect upon the excitability of the α-motoneurons.

In conclusion, we have revealed specific distributions of the α1 and α3 subunits of NKA throughout the spinal cord. The difference in the distribution of these isoforms is highlighted in the ventral horn, where the NKAα1 subunit is found within α-motoneurons and the NKAα3 subunit within γ-motoneurons. Electrophysiological experiments confirmed the mutually exclusive distribution of the NKAα subunits in motoneurons. Such differential distribution has consequences for physiological function of sensorimotor circuits and may contribute to symptoms of pathophysiological mutations in NKAα3.

References

Arber S, Ladle DR, Lin JH, Frank E, Jessell TM (2000) ETS gene Er81 controls the formation of functional connections between group Ia sensory afferents and motor neurons. Cell 101:485–498. CrossRef Medline

Arystarkhova E, Sweadner KJ (1996) Isoform-specific monoclonal antibodies to Na,K-ATPase alpha subunits. Evidence for a tissue-specific post-translational modification of the alpha subunit. J Biol Chem 271:23407–23417. CrossRef Medline

Azarias G, Kruusmägi M, Connor S, Akkuratov EE, Liu XL, Lyons D, Brismar H, Broberger C, Aperia A (2013) A specific and essential role for Na,K-ATPase alpha3 in neurons co-expressing alpha1 and alpha3. J Biol Chem 288:2734–2743. CrossRef Medline

Brashear A, Butler IJ, Ozelius LJ, Kramer PI, Farlow MR, Breakefield XO, Dobyns WB (1998) Rapid-onset dystonia-parkinsonism: a report of clinical, biochemical, and genetic studies in two families. Adv Neurol 78:335–339. Medline

Brashear A, Dobyns WB, de Carvalho Aguiar P, Borg M, Frijns CJ, Gollamudi S, Green A, Guimaraes J, Haake BC, Klein C, Linazasoro G, Münchau A, Raymond D, Riley D, Saunders-Pullman R, Tijssen MA, Webb D, Zaremba J, Bressman SB, Ozelius LJ (2007) The phenotypic spectrum of rapid-onset dystonia-parkinsonism (RDP) and mutations in the ATP1A3 gene. Brain 130:828–835. CrossRef Medline

Calderon DP, Fremont R, Kraenzlin F, Khodakhah K (2011) The neural substrates of rapid-onset Dystonia-Parkinsonism. Nat Neurosci 14:357–365. CrossRef Medline

de Carvalho Aguiar P, Sweadner KJ, Penniston JT, Zaremba J, Liu L, Caton M, Linazasoro G, Borg M, Tijssen MA, Bressman SB, Dobyns WB, Brashear A, Ozelius LJ (2004) Mutations in the NKA alpha 3 gene ATP1A3 are associated with rapid onset dystonia parkinsonism. Neuron 43:169–175. CrossRef Medline

Deutschländer A, Asmus F, Gasser T, Steude U, Bötzel K (2005) Sporadic rapid-onset dystonia-parkinsonism syndrome: failure of bilateral pallidal stimulation. Mov Disord 20:254–257. CrossRef Medline

Dobretsov M, Hastings SL, Stimers JR (1999) Non-uniform expression of alpha subunit isoforms of the Na+/K+ pump in rat dorsal root ganglia neurons. Brain Res 821:212–217. CrossRef Medline

Dobretsov M, Hastings SL, Sims TJ, Stimers JR, Romanovsky D (2003) Stretch receptor-associated expression of alpha 3 isoform of the Na+, K+-ATPase in rat peripheral nervous system. Neuroscience 116:1069–1080. CrossRef Medline

Edwards IJ, Dallas ML, Poole SL, Milligan CJ, Yanagawa Y, Szabó G, Erdélyi F, Deuchars SA, Deuchars J (2007) The neurochemically diverse intermedius nucleus of the medulla as a source of excitatory and inhibitory syn-

aptic input to the nucleus tractus solitarii. J Neurosci 27:8324–8333. CrossRef Medline

Ellaway PH, Murphy PR (1981) A comparison of the recurrent inhibition of alpha- and gamma-motoneurones in the cat. J Physiol 315:43–58. Medline

Enjin A, Leão KE, Mikulovic S, Le Merre P, Tourtellotte WG, Kullander K (2012) Sensorimotor function is modulated by the serotonin receptor 1d, a novel marker for gamma motor neurons. Mol Cell Neurosci 49:322–332. CrossRef Medline

Friese A, Kaltschmidt JA, Ladle DR, Sigrist M, Jessell TM, Arber S (2009) Gamma and alpha motor neurons distinguished by expression of transcription factor Err3. Proc Natl Acad Sci U S A 106:13588–13593. CrossRef Medline

Giuffrida R, Rustioni A (1992) Dorsal root ganglion neurons projecting to the dorsal column nuclei of rats. J Comp Neurol 316:206–220. Medline

Harwood S, Yaqoob MM (2005) Ouabain-induced cell signaling. Front Biosci 10:2011–2017. CrossRef Medline

Heinzen EL, Swoboda KJ, Hitomi Y, Gurrieri F, Nicole S, de Vries B, Tiziano FD, Fontaine B, Walley NM, Heavin S, Panagiotakaki E, European Alternating Hemiplegia of Childhood (AHC) Genetics Consortium, Biobanca e Registro Clinico per l'Emiplegia Alternante (I.B.AHC) Consortium, European Network for Research on Alternating Hemiplegia (ENRAH) for Small and Medium-sized Enterpriese (SMEs) Consortium, Fiori S, Abiusi E, Di Pietro L, Sweney MT, Newcomb TM, Viollet L, et al. (2012) De novo mutations in ATP1A3 cause alternating hemiplegia of childhood. Nat Genet 44:1030–1034. CrossRef Medline

Ichikawa H, Mo Z, Xiang M, Sugimoto T (2004) Effect of Brn-3a deficiency on parvalbumin-immunoreactive primary sensory neurons in the dorsal root ganglion. Brain Res Dev Brain Res 150:41–45. CrossRef Medline

Kirshenbaum GS, Dawson N, Mullins JG, Johnston TH, Drinkhill MJ, Edwards IJ, Fox SH, Pratt JA, Brotchie JM, Roder JC, Clapcote SJ (2013) Alternating hemiplegia of childhood-related neural and behavioural phenotypes in Na(+),K(+)-ATPase alpha3 missense mutant mice. PloS one 8:e60141. CrossRef Medline

Kulkarni V, Chandy MJ, Babu KS (2001) Quantitative study of muscle spindles in suboccipital muscles of human foetuses. Neurol India 49:355–359. Medline

Mata M, Siegel GJ, Hieber V, Beaty MW, Fink DJ (1991) Differential distribution of (Na,K)-ATPase alpha isoform mRNAs in the peripheral nervous system. Brain Res 546:47–54. CrossRef Medline

McGrail KM, Phillips JM, Sweadner KJ (1991) Immunofluorescent localization of three Na,K-ATPase isozymes in the rat central nervous system: both neurons and glia can express more than one Na,K-ATPase. J Neurosci 11:381–391. Medline

Mentis GZ, Siembab VC, Zerda R, O'Donovan MJ, Alvarez FJ (2006) Primary afferent synapses on developing and adult Renshaw cells. J Neurosci 26:13297–13310. CrossRef Medline

O'Brien WJ, Lingrel JB, Wallick ET (1994) Ouabain binding kinetics of the rat alpha two and alpha three isoforms of the sodium-potassium adenosine triphosphate. Arch Biochem Biophys 310:32–39. CrossRef Medline

Richmond FJ, Abrahams VC (1975) Morphology and distribution of muscle spindles in dorsal muscles of the cat neck. J Neurophysiol 38:1322–1339. Medline

Romanovsky D, Moseley AE, Mrak RE, Taylor MD, Dobretsov M (2007) Phylogenetic preservation of alpha3 Na+,K+-ATPase distribution in vertebrate peripheral nervous systems. J Comp Neurol 500:1106–1116. CrossRef Medline

Rosewich H, Thiele H, Ohlenbusch A, Maschke U, Altmüller J, Frommolt P, Zirn B, Ebinger F, Siemes H, Nürnberg P, Brockmann K, Gärtner J (2012) Heterozygous de-novo mutations in ATP1A3 in patients with alternating hemiplegia of childhood: a whole-exome sequencing gene-identification study. Lancet Neurol 11:764–773. CrossRef Medline

Sayers ST, Khan T, Shahid R, Dauzvardis MF, Siegel GJ (1994) Distribution of alpha 1 subunit isoform of (Na,K)-ATPase in the rat spinal cord. Neurochem Res 19:597–602. CrossRef Medline

Segall L, Daly SE, Blostein R (2001) Mechanistic basis for kinetic differences between the rat alpha 1, alpha 2, and alpha 3 isoforms of the Na,K-ATPase. J Biol Chem 276:31535–31541. CrossRef Medline

Shneider NA, Brown MN, Smith CA, Pickel J, Alvarez FJ (2009) Gamma motor neurons express distinct genetic markers at birth and require muscle spindle-derived GDNF for postnatal survival. Neural Dev 4:42. CrossRef Medline

Shyjan AW, Levenson R (1989) Antisera specific for the alpha 1, alpha 2, alpha 3, and beta subunits of the Na,K-ATPase: differential expression of alpha and beta subunits in rat tissue membranes. Biochemistry 28:4531–4535. CrossRef Medline

Strick PL, Burke RE, Kanda K, Kim CC, Walmsley B (1976) Differences between alpha and gamma motoneurons labeled with horseradish peroxidase by retrograde transport. Brain Res 113:582–588. CrossRef Medline

Sweadner KJ (1989) Isozymes of the Na+/K+-ATPase. Biochim Biophys Acta 988:185–220. CrossRef Medline

Urayama O, Sweadner KJ (1988) Ouabain sensitivity of the alpha 3 isozyme of rat Na,K-ATPase. Biochem Biophys Res Commun 156:796–800. CrossRef Medline

Viola MS, Rodríguez de Lores Arnaiz G (2007) Brain Na+, K+-ATPase isoforms: different hypothalamus and mesencephalon response to acute desipramine treatment. Life Sci 81:228–233. CrossRef Medline

Wang L, Spary E, Deuchars J, Deuchars SA (2008) Tonic GABAergic inhibition of sympathetic preganglionic neurons: a novel substrate for sympathetic control. J Neurosci 28:12445–12452. CrossRef Medline

Watts AG, Sanchez-Watts G, Emanuel JR, Levenson R (1991) Cell-specific expression of mRNAs encoding Na+,K(+)-ATPase alpha- and beta-subunit isoforms within the rat central nervous system. Proc Natl Acad Sci U S A 88:7425–7429. CrossRef Medline

Westbury DR (1982) A comparison of the structures of alpha and gamma-spinal motoneurones of the cat. J Physiol 325:79–91. Medline